

# **Negative Refraction and Left-handed electromagnetism in Microwave Photonic Crystals**

P. V. Parimi, W. T. Lu, P. Vodo, J. Sokoloff, and S. Sridhar\*

Department of Physics and Electronic Materials Research Institute, Northeastern  
University, 360 Huntington Avenue, Boston, MA 02115.

We demonstrate negative refraction of microwaves in metallic photonic crystals. The spectral response of the photonic crystal, which manifests both positive and negative refraction, is in complete agreement with band-structure calculations and numerical simulations. The negative refraction observed corresponds to left-handed electromagnetism and arises due to the dispersion characteristics of waves in a periodic medium. This mechanism for negative refraction is different from that in metamaterials.

78.20.Ci, 42.70.Qs, 41.20.Jb

The optical properties of materials that are transparent to electromagnetic (EM) waves can be characterized by an index of refraction  $n$ . Given the direction of the incident beam  $\theta_1$  at the interface of vacuum and the material, the direction  $\theta_2$  of the outgoing beam can be determined using Snell's formula  $\sin\theta_1 = n \sin\theta_2$ . All naturally available materials possess a positive refractive index  $n > 0$ . It was observed recently that in certain composite metamaterials EM waves bend negatively<sup>1</sup> and consequently a negative index of refraction  $n < 0$  can be assigned to such materials without violating Maxwell's equations. For homogeneous media, negative refraction ( $\theta_2 < 0, \theta_1 > 0$ ) necessarily requires that  $n < 0$ . This negative bending allows considerable control over light propagation and opens the door for new approaches to a variety of applications from microwave to optical frequencies.

Negative index media exhibit some unusual propagation characteristics of EM waves. The most striking property is that of Left-Handed Electromagnetism (LHE) since the electromagnetic fields  $\vec{E}$  and  $\vec{H}$ , and the wave vector  $\vec{k}$  form a left-handed triplet set. Consequently the energy flow represented by the Poynting vector  $\vec{S} = \vec{E} \times \vec{H}$  is anti-parallel to the wave vector  $\vec{k}$ , so that  $\vec{S} \cdot \vec{k} < 0$ . In contrast for conventional  $n > 0$  materials  $\vec{E}, \vec{H}, \vec{k}$  form a right-handed set corresponding to Right-Handed Electromagnetism (RHE), and  $\vec{S} \cdot \vec{k} > 0$ .

A material possessing simultaneously negative permittivity  $\varepsilon < 0$  and permeability  $\mu < 0$  can be shown to necessarily have  $n \equiv \sqrt{\varepsilon\mu} = -\sqrt{|\varepsilon||\mu|} < 0$ <sup>2,3</sup>. Recently, negative refraction was demonstrated in a quasi-homogeneous metamaterial<sup>1,4</sup> with unit cell dimensions less than the wavelength, consisting of interleaved arrays of wires ( $\varepsilon < 0$ ) and split ring resonators ( $\mu < 0$ ). However the physical reality of negative refraction in these materials has been questioned<sup>5</sup>. Furthermore these materials are highly absorptive, and unlikely to be scaled to three dimensions or to smaller sizes suitable for applications at optical frequencies<sup>1,6</sup>.

It has since been proposed that negative refraction can be achieved in photonic crystals (PC), which are inhomogeneous periodic media with lattice constant comparable to the wavelength<sup>6,7,8</sup>. A PC is an artificial structure, usually made of a dielectric or metal, designed to control photons similar to the way a solid state crystal controls electrons. Locally both  $\varepsilon, \mu > 0$  everywhere in the PC. The physical principles that allow negative refraction in the PC arise from the dispersion characteristics of wave propagation in a periodic medium, and are very different from that of the metamaterial in Ref. [1]. In this Letter we present experimental evidence of negative refraction of microwaves in a metallic photonic crystal. Parallel theoretical and numerical investigations of the band structure and simulations of wave propagation through the PC prism are compared with the experimental results. Exceptionally good agreement is found between the experiments, band structure calculations and wave refraction simulations.

The microwave photonic crystal fabricated in the present work is an array of cylindrical copper rods of height 1.26 cm and radius 0.63 cm forming a triangular or square lattice. The ratio of the radius  $r$  to lattice constant  $a$  is kept at  $r/a = 0.2$ . Refraction measurements are carried out in a parallel plate waveguide made of a pair of metallic plates. A coax-to-waveguide adaptor is employed to couple microwave radiation into the parallel plate waveguide. The excitation in the parallel plate waveguide is transverse magnetic (TM) mode up to 12 GHz such that the electric field  $\vec{E}$  is parallel to the axis of the rods. Microwave absorbers are placed on either side to collimate the propagating beam and to avoid spurious reflections. The collimated microwave beam propagates a distance of 90 cm in the waveguide, and then is incident normally to and at the center of the longer side of a right angle prism of PC (see Fig. 1).

The other face of the prism, which is the surface of refraction, is at  $60^\circ$  to the incident beam, such that the angle between the normal to the surface and incident beam is  $30^\circ$ . A dipole antenna is mounted on a goniometer that runs along the semicircular outer edge of the parallel plate waveguide to detect the refracted beam. The detector is positioned at 25 cm

from the refraction surface to eliminate near field effects and possible interference with fields inside the PC. The refraction is considered positive (negative) if the emerging beam is detected at positive (negative) angles as shown in Fig. 1.

The refraction experiment is validated by data on a PTFE (Teflon) prism having the same dimensions as that of the PC prisms. Fig 1(b) shows the transmitted intensity  $|S_{21}|^2$  versus angle  $\theta$  from the normal to the refracting surface of the prism. A peak is clearly seen at  $\theta_2 = +45^\circ$  corresponding to a positive refractive index  $n = 1.4$  ( $n \sin \theta_1 = \sin \theta_2$ ) for an incident angle  $\theta_1 = 30^\circ$ . The refraction angle is frequency independent in the current spectral region of interest 5.5-12 GHz, consistent with a frequency-independent refractive index expected for Teflon.

The measurements on the triangular PC were carried out with the incident wave vector  $\vec{k}_i$  along directions  $\Gamma \rightarrow K$  and  $\Gamma \rightarrow M$  of the first Brillouin zone (these directions in real space and in reciprocal wave-vector space are shown in Fig. 3(a) and 3(b)). Fig. 1(b) illustrates the plot of intensity  $|S_{21}|^2$  vs.  $\theta$  at 8.63 GHz for the microwave beam incident along the  $\Gamma \rightarrow K$  direction. A strong peak can be seen around  $-35^\circ$  which represents negative refraction by the PC prism. Using Snell's law,  $\sin \theta_2 = n_{\text{eff}} \sin \theta_1$  with  $\theta_1 = 30^\circ$ ,  $\theta_2 = -35^\circ$ , we obtain an *effective* refractive index of  $n_{\text{eff}} = -1.15$  for the PC at 8.63 GHz. A second low intensity peak can also be seen at  $-80^\circ$  which is likely to be an edge effect. The negative refraction reported in the present photonic crystal has been demonstrated for the first time in an inhomogeneous system.

A complete spectrum of transmission data covering the frequency region 5.5 to 12 GHz and angles from  $-90^\circ$  to  $+90^\circ$  is shown in Fig. 2(a). For better color contrast, the data are represented in terms of the transmission amplitude  $|\tilde{S}_{21}|$ . The data are strongly frequency dependent, unlike similar data for Teflon (not shown). As can be seen from the figure below 6.2 GHz the transmission through the PC is negligible. Between 6.2 GHz and 7.7 GHz largely positive refraction is observed with maximum intensity around  $+10^\circ$ . This is followed by a region of negative refraction with maximum intensity around  $-35^\circ$  between 7.7 and 11.1 GHz. In the region above 11.1 GHz the emerging beam is found to be quite weak.

An understanding of negative refraction and its relation to left-handed behavior of electromagnetic waves in a photonic crystal can be achieved by examining the band structure of an infinite PC. We have calculated the band structure employing standard plane wave expansion methods using over 2000 plane waves<sup>9</sup>. The 2D band structure for a triangular lattice PC with  $r/a = 0.2$  is shown in Fig. 3(c).

For a plane wave with wave vector  $\vec{k}_i$  and frequency  $\omega$  incident normal to an air-PC interface, the wave vector  $\vec{k}_f$  inside the PC is parallel or anti-parallel to  $\vec{k}_i$  as determined by the band structure. If  $d\omega/d|\vec{k}_f| > 0$ ,  $\vec{k}_f$  is parallel to  $\vec{k}_i$  and consequently the EM field in PC is right-handed (RHE). Otherwise,  $\vec{k}_f$  is anti-parallel to  $\vec{k}_i$  and the EM field in the PC is left-handed (LHE). For a general case the phase and group velocities in a medium are  $\vec{v}_p = (c/|n_p|)\hat{k}_f$ , with  $\hat{k}_f = \vec{k}_f / k_f$ , and  $|\vec{v}_g| = |\nabla_k \omega| = c/|n_g|$ . An effective refractive index can be defined  $n_p = \text{sgn}(\vec{v}_g \cdot \vec{k}_f) \frac{c|\vec{k}_f|}{\omega}$  and calculated from the band structure<sup>10</sup>. The sign of  $n_p$  is determined from the behavior of the equi-frequency surfaces (EFS). EFS plots for the first and second bands of the triangular lattice are shown in Fig. 3(b). The center in the plots corresponds to the center of the first Brillouin zone. The EFS that move outwards from the center with increasing frequency correspond to RHE with  $\vec{v}_g \cdot \vec{k}_f > 0$  and inward moving surfaces correspond to LHE with  $\vec{v}_g \cdot \vec{k}_f < 0$ . In the case of LHE (RHE) conservation of  $\vec{k}_f$  component along the surface of refraction would result in negative (positive) refraction.

The resulting refractive index  $n_p$  determined from the band structure and EFS for a beam incident along  $\Gamma \rightarrow K$  is shown in Fig. 2(b). Negative refraction is predicted for regions in the 2<sup>nd</sup> and 3<sup>rd</sup> bands and positive refraction in the 1<sup>st</sup> and 4<sup>th</sup> bands.

The notion of an effective index of refraction  $n_p$  discussed above has limited validity in a PC which is intrinsically inhomogeneous. In certain frequency ranges which are far away from the RHE  $\leftrightarrow$  LHE transition points it can be used in Snell's law to approximately determine the direction of propagation. The strong dispersion and anisotropy means that the nature of refraction in arbitrary directions can be quite complicated and leads to some additional interesting possibilities <sup>6</sup>. However it can be proved analytically that the direction of group velocity  $\vec{v}_g$  in an infinite PC coincides with that of the energy flow  $\vec{S}$  <sup>11</sup>.

The experimental results of refraction (Fig 2(a)) are remarkably consistent with the results deduced from the band structure calculations (Fig 2(b)). In Fig 2(c) a few illustrative experimental results that show negative and positive refraction in different frequency ranges are presented.

- (I) In the first band between 6.2 – 7.7 GHz the EFS move outward with increasing frequency, so that  $n_p > 0$  corresponding to RHE with  $\vec{v}_g \cdot \vec{k}_f > 0$  (i.e  $\vec{v}_g$  parallel to  $\vec{k}_f$ ). The representative plot at  $f = 7.32$  GHz in Fig. 2.(c) shows that the signal is largely in the positive direction.
- (II) In the second band between 7.7 – 11 GHz, the EFS move inward with increasing frequency, consistent with  $n_p < 0$  corresponding to LHE with  $\vec{v}_g \cdot \vec{k}_f < 0$  (  $\vec{v}_g$  anti-parallel to  $\vec{k}_f$  ). Two illustrative plots in Fig. 2(c) corresponding to 8.5 and 9.54 GHz show that the signal is strongly peaked in the negative direction.
- (III) A band gap is clearly observed in the experiment, which matches with the band structure, in the region between 11.13-11.32 GHz. As can be seen from the figure the transmission through the PC is near zero. At lower frequencies, transmission starts at around 6.2 GHz above the band cutoff and close to the onset of the first band predicted by the calculations.

We have also examined the nature of the modes inside the PC. For the frequencies considered here, it appears likely that there is some variation of the wave function in directions perpendicular to  $\vec{k}_f$  and hence a single beam is not achieved. A single beam may be possible for frequencies below 7.5 GHz, although there the refraction is positive.

A noteworthy feature is that the  $|S_{21}|^2$  transmission peak for the PC prism is nearly 400% of that of an identical Teflon prism (Fig. 1b). In comparison a homogeneous negative index metamaterial shows a refraction peak 4% in intensity ( 20% in electric field ) of that of Teflon <sup>4, 12</sup>. Thus the attenuation in the PC prism is nearly 100 times smaller than that in a comparable prism made of the negative index metamaterial. This is crucial for applications such as imaging. Another significant feature of the PC data is the narrowness of the peak which suggests intense focusing resulting from the resonant interactions of EM waves with the metallic PC.

Similar results are also observed for a square lattice metallic PC. We find large spectral regions of negative refraction consistent with band-structure calculations.

Direct numerical simulations (see Fig.4) of wave refraction were carried out and are in good agreement with the experimental results and band-structure calculations. The simulation is done using a Green's function boundary wall

approach (GBW) originally developed for hard wall potentials in quantum mechanics <sup>13</sup>. Consider a  $\delta$ -type potential  $V(\vec{r}) = \gamma \int_C ds \delta(\vec{r} - \vec{r}(s))$  with boundary  $C$  divided into  $N$  parts so that each part  $C_j$  has length  $\Delta_j$ . For an incident initial wave function  $\phi(\vec{r})$  and  $k\Delta_j \ll 1$ , the wave function on  $C_j$  can be assumed to be constant. The resultant wave function is  $\psi(\vec{r}) \approx \phi(\vec{r}) + \gamma \sum_{j=1}^N \int_{C_j} ds G_0(\vec{r}, \vec{r}(s)) \psi(\vec{r}_j)$ . Here  $G_0(\vec{r}, \vec{r}')$  is the free space Green's function. Defining a matrix  $M_{ij} = \int_{C_j} ds G_0(\vec{r}_i, \vec{r}(s))$ , one gets  $\psi(\vec{r}_i) = (1 - \gamma M)^{-1} \phi(\vec{r}_j)$ . In the limit  $\gamma \rightarrow \infty$  the wave function  $\psi(\vec{r})$  will vanish on the boundary and one has

$$\psi(\vec{r}) = \phi(\vec{r}) - \sum_{j=1}^N G_0(\vec{r}, \vec{r}_j) \Delta_j (M^{-1} \Phi)_j$$

with  $\Phi = (\phi(\vec{r}_1), \dots, \phi(\vec{r}_N))$ . As shown in Fig. 4, the GBW simulation results in negative refraction for  $f = 9.0$  GHz in the 2<sup>nd</sup> band, and positive refraction for  $f = 7.0$  GHz in the 1<sup>st</sup> band, both in agreement with the experiment (Fig. 2).

In conclusion we have experimentally demonstrated negative refraction in a new class of materials, metallic photonic crystals. The present work demonstrates the physical reality of negative refraction and its association with left-handed electromagnetism, thereby refuting the questions raised <sup>5</sup>.

A major feature of the present work is the extraordinary level of control exemplified by the convergence between the experimental data, band structure calculations and GBW simulations. This means that a variety of tailor-made structures are feasible that can be designed and constructed. There are numerous possibilities opened up by the present results. For many applications such as imaging, one requires index matching between the negative index material and surroundings (relative index  $n = -1$ ) accompanied by negligible losses. These requirements are more easily met with PC than with composite negative index metamaterials. Metallic PC offers the additional advantages of the highest dielectric contrast, low attenuation and the possibility of focusing, which are evident from the present data. Furthermore the microwave PC can be easily scaled to 3 dimensions<sup>14</sup>, and to optical frequencies which is highly unlikely with composite negative index metamaterials <sup>1,6</sup>. Thus the advantages of negative refraction and left-handed electromagnetism that have been proposed recently, such as imaging by flat lenses <sup>15</sup>, beam steerers, couplers and others, as well as some entirely new possibilities, are feasible with photonic crystals from microwave to optical frequencies.

Work supported by the National Science Foundation and the Air Force Research Laboratories.

\*Electronic address: s.sridhar@neu.edu

**Fig.1. (a) Schematic diagram of the microwave refraction experimental setup. (b) Microwave transmission intensity  $|S_{21}|^2$  vs. angle at  $f = 8.63\text{GHz}$ . Negative refraction is clearly observed for the photonic crystal prism. An identical Teflon prism shows positive refraction.**

**Fig 2. [Color] (a) Microwave transmission amplitude  $|S_{21}|$  vs. frequency  $f$  (GHz) and angle  $\theta$  for the PC prism. Note negative refraction (NR) in the region 7.7-11 GHz and positive refraction (PR) between 6.3-7.7 GHz. (b) Refractive index  $n_p$  for different frequencies of a beam incident along the  $\Gamma \rightarrow K$  direction calculated from the band structure and EFS. For  $n_p < 0$  ( $n_p > 0$ ), the electromagnetism is left-handed (right-handed), and the refraction angle is negative (positive). The close match between the experimental data and the behavior of  $n_p$  is evident. (c) Representative plots of transmission intensity  $|S_{21}|^2$  for positive and negative refraction, as well as band gap regions.**

**Fig.3. [Color] (a) Propagation vectors for positive and negative refraction.  $k_t$  is the wave vector of the refracted beam. (b) The EFS for the 1<sup>st</sup> and 2<sup>nd</sup> bands. The centers of the hexagons represent the centers of the first Brillouin zones in the respective bands. Blue (red) color represents lower (higher) frequency. (c) Band structure computed for the triangular lattice metallic PC with  $r/a = 0.2$ .**

**Fig. 4. [Color] Simulations of wave refraction showing the wave front emerging from a metallic PC: (a) Positive refraction at 7.0 GHz and (b) negative refraction at 9.0 GHz. The PC used in the simulations has the same size as that used in the experiment. The electric field is plotted as  $E_z^{1/3}$  for better visibility.**

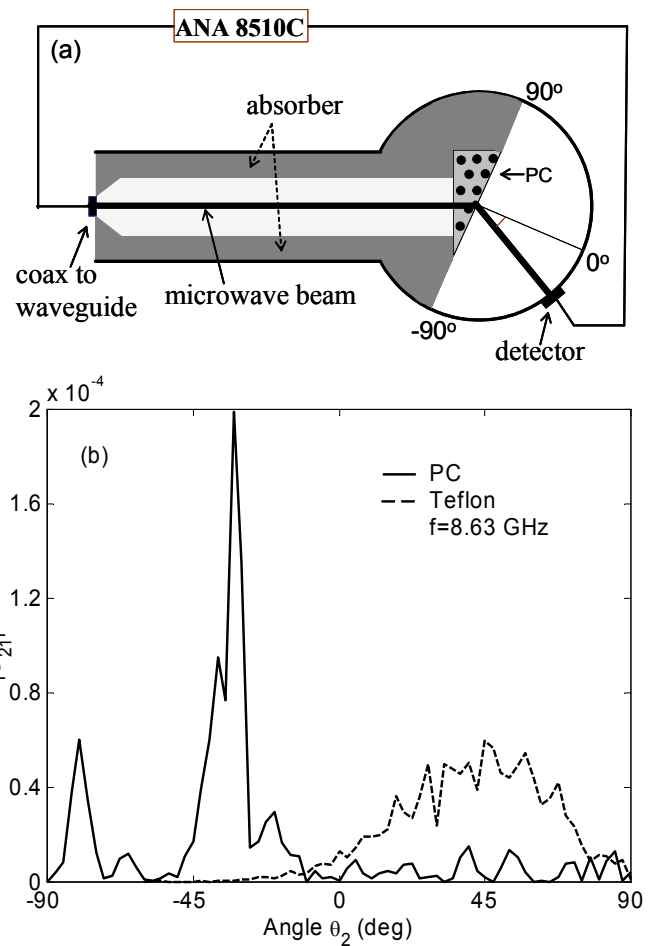


Fig. 1 – Parimi et al.

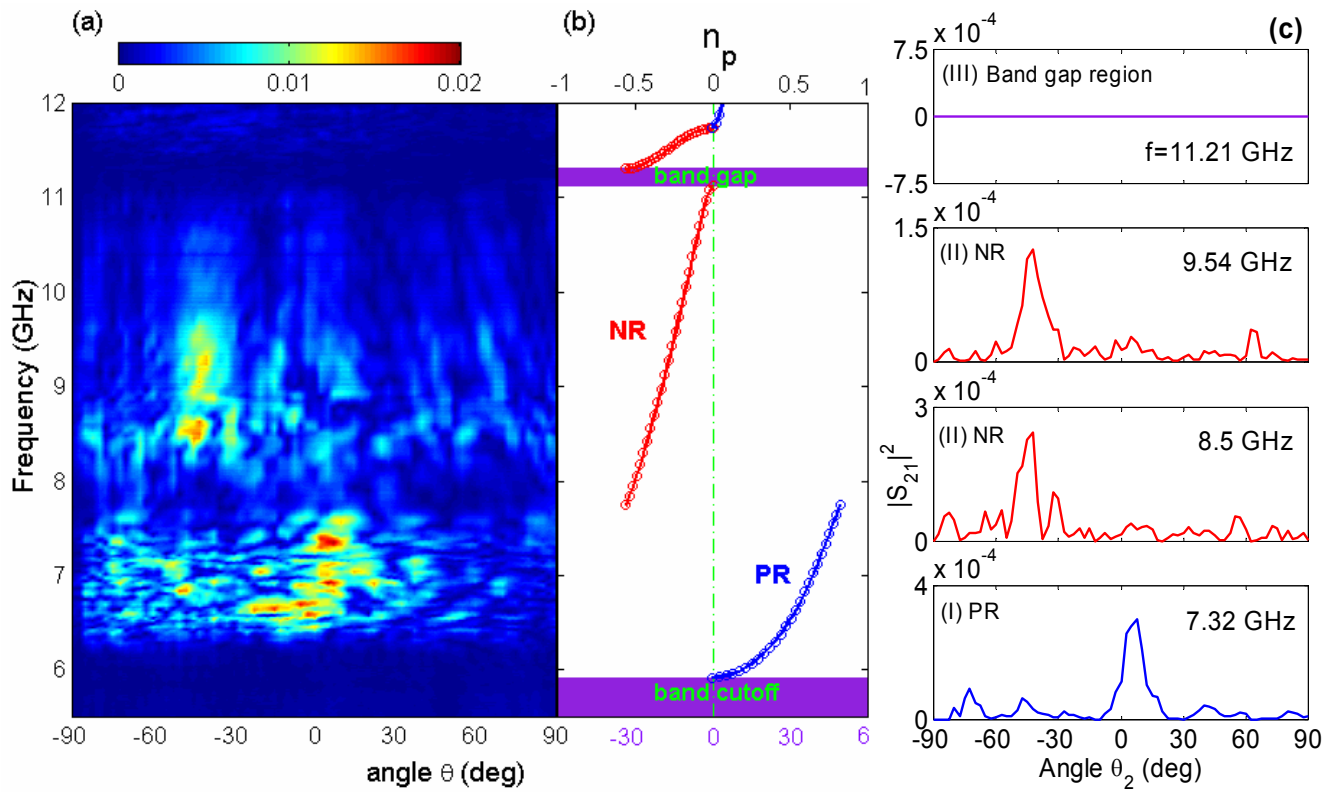


Fig. 2 – Parimi et al.

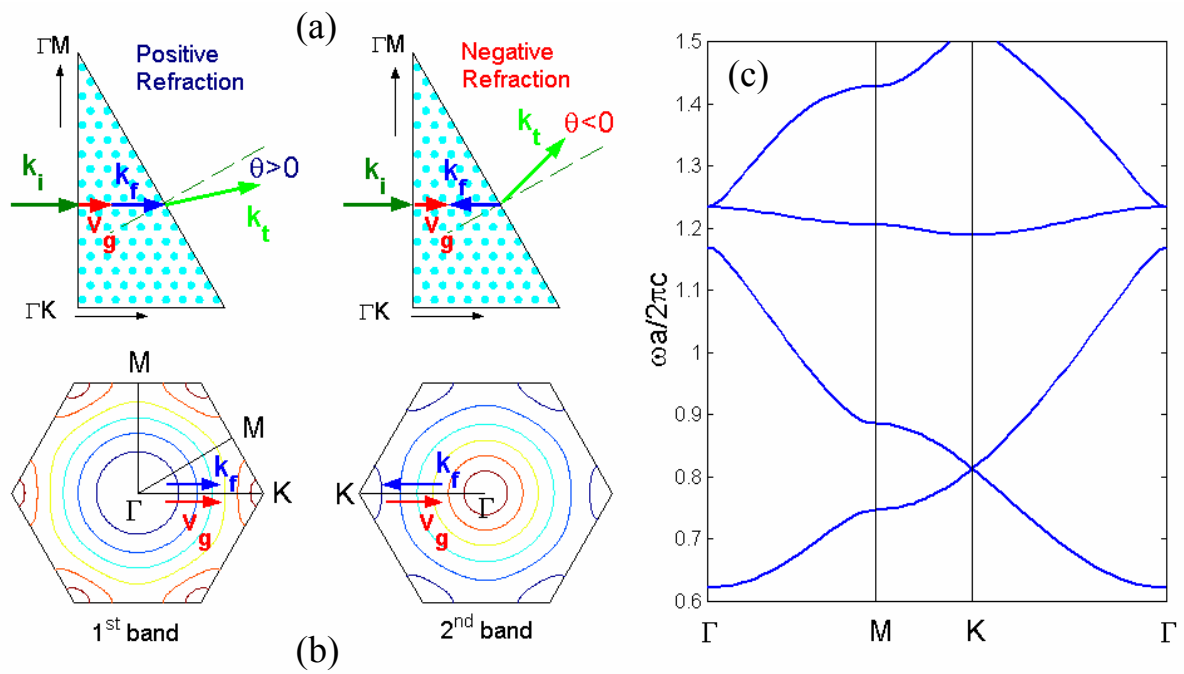


Fig. 3 – Parimi et al.

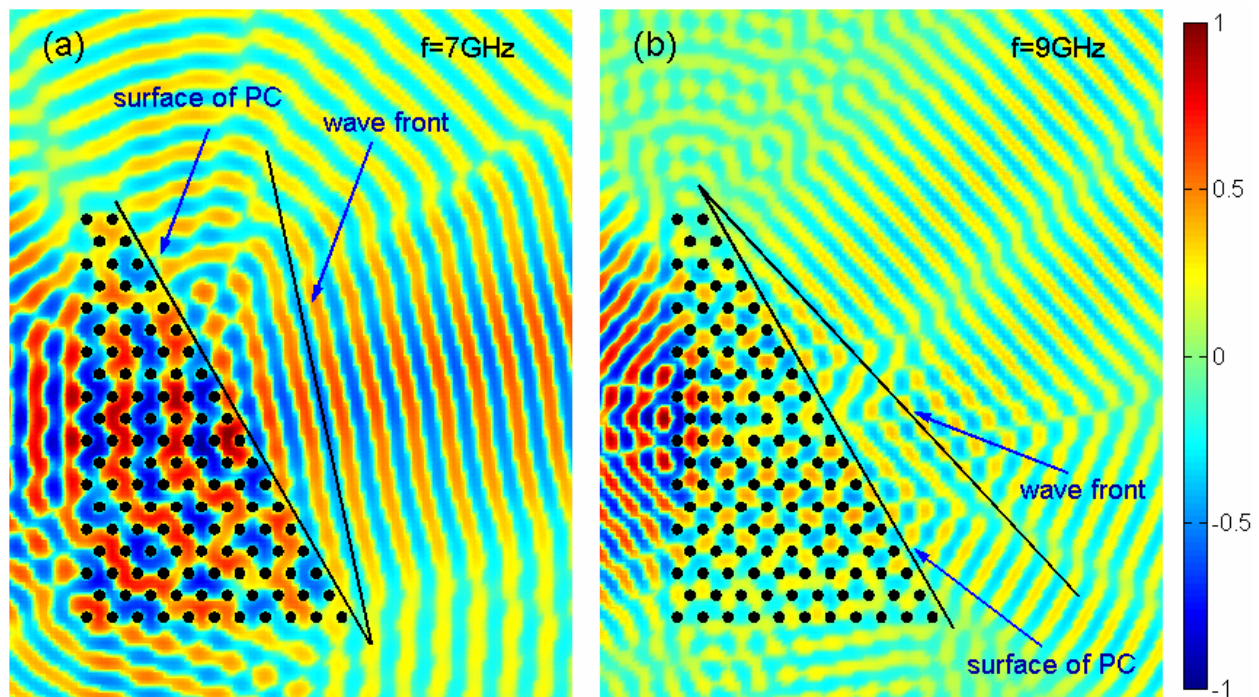


Fig 4 – Parimi et al.

---

<sup>1</sup> R. A. Shelby, D. R. Smith, and S. Schultz, *Science* **77**, 292 (2001).

<sup>2</sup> V. Veselago, *Soviet Physics USPEKHI* **10**, 509 (1968).

<sup>3</sup> D. R. Smith and N. Kroll, *Phys. Rev. Lett.* **85**, 3966 (2000).

<sup>4</sup> C. G. Parazzoli, R. B. Gregor, K. Li, B. E. C. Koltenbach, and M. Tanielian, *Phys. Rev. Lett.* **90**, 107401 (2003).

<sup>5</sup> P. M. Valanju, R. M. Walser, and A. P. Valanju, *Phys. Rev. Lett.* **88**, 187401 (2002).

<sup>6</sup> C. Luo, S.G. Johnson, J. D. Joannopoulos, and J. B. Pendry, *Phys. Rev. B* **65**, 201104 (2002).

<sup>7</sup> M. Notomi, *Phys. Rev. B* **62**, 10696 (2002).

<sup>8</sup> H. Kosaka, et al., *Phys. Rev. B* **58**, R10096 (1998).

<sup>9</sup> W. T. Lu and S. Sridhar, to be published

<sup>10</sup> S. Foteinopoulou and C.M Soukoulis, arXiv: cond-mat/0212434 (2002)

<sup>11</sup> K. Sakoda, *Optical properties of photonic crystal* (Springer, 2001)

<sup>12</sup> P.V. Parimi, P. Vodo, W.T. Lu, J. S. Derov, B.Turchinets and S. Sridhar, to be published

<sup>13</sup> M. G. E. Da Luz, A. S. Lupu-Sax, and E. J. Heller, *Phys. Rev. E* **56**, 2496 (1997).

<sup>14</sup> D. F. Sievenpiper, M. E. Sickmiller, and E. Yablonovitch, *Phys. Rev. Lett.* **76**, 2480 (1996).

<sup>15</sup> J. B. Pendry, *Phys. Rev. Lett.* **85**, 3966 (2000).